Liquid/Vapor Surface Tension of Metals: Embedded Atom Method with Charge Gradient Corrections

Edmund B. Webb III and Gary S. Grest
Sandia National Laboratory, Albuquerque, New Mexico 87185-1411
(Received 20 April 2000)

Molecular dynamics simulations for three embedded atom method (EAM) function sets are used to determine the liquid/vapor surface tension γ for Al, Ni, Cu, Ag, and Au. The three EAM models differ in both the functional forms employed and the fitting procedure used. All the EAM potentials underestimate γ but one of the models performs consistently better than the others. We show that including a correction to the local charge density associated with gradients in the density together with exploiting the invariance of the EAM potentials to appropriate transformations in the charge density can lead to improved values for γ, as well as for solid free surface energies, within existing EAM function sets.

DOI: 10.1103/PhysRevLett.86.2066 PACS numbers: 68.03.Cd, 02.70.Ns, 68.03.Hj, 68.35.Md

A popular model for performing atomistic simulations of metals is the embedded atom method (EAM) which incorporates a multibody contribution to the energy of an atom. The EAM overcomes deficiencies in pair potentials used for simulating metals [1]; it has origins in density-functional theory but is an empirical potential which is only slightly more difficult to implement than a pair potential. Much work exists toward applying the EAM to study bulk, surface, point defect, and alloy behavior [1]. This method has also been used to study properties of liquid metals [2]. A shortcoming of many parametrizations within the EAM is significant underprediction of surface energetics in both the solid and the liquid states [1,2]. While the simplicity of the EAM makes it an attractive option for large scale interface simulations, surface energy predictions must be rectified before trusting quantitative results from such simulations.

The energy of a system of N atoms in the EAM is

$$E_s = \sum_{i=1}^{N} \left[F_i(\rho_i) + \frac{1}{2} \sum_{j \neq i} \phi_{ij}(R) \right]. \tag{1}$$

Here ρ_i is the local charge density at atom i,

$$\rho_i = \sum_{j \neq i} \rho_j^a(R), \tag{2}$$

where $\rho_j^a(R)$ is the spherically symmetric electron density contributed by atom j, a distance R from i. $F_i(\rho_i)$ is the energy associated with embedding atom i into an electron density ρ_i, and $\phi_{ij}(R)$ is a pair potential between atoms i and j. There is no single way to determine $\rho_i^a(R)$, $\phi_{ij}(R)$, and $F_i(\rho_i)$, but a typical approach is to assume some physically appropriate mathematical forms and fit the resulting parameters to experimentally measured material properties. Most function sets have been developed using only bulk experimental data or, if surface data were included, they were not highly weighted in the fit. This is one reason why most EAM parametrizations do not perform well when used to quantitatively predict surface properties where charge densities are significantly different from the bulk.

One way to improve EAM surface predictions is to fit new potential functions to experimental surface data; however, this risks achieving less success in bulk thermodynamic predictions. By using the modified EAM (which incorporates angular dependence of the atomic charge density into the model), one group predicted relaxed solid free surface energy for eight metals [3], five of which are addressed here. For every case except Ni, the modified EAM predictions were 10%–30% less than experiment. In addition, many more functions exist for the standard EAM so it is useful to investigate ways of reconciling their surface prediction accuracy. A method [4] that has been demonstrated to work for one EAM model of Au [5] involves adding corrections to the argument of F_i related to the nonuniformity in the charge density,

$$F_i(\rho_i) \rightarrow F_i(\rho_i + \alpha \nabla^2 \rho_i + \beta |\nabla \rho_i|^2). \tag{3}$$

Density-functional theory demonstrates that these are the lowest order terms in charge nonuniformity upon which the embedding energy depends [4]. For Au, Roelofs *et al.* [5] assumed $\alpha = 0$ and identified a range of β that corrected inaccurate predictions of the relative stability of the (1×1), (1×2), and (1×3) reconstructions on the (110) surface. As in Ref. [5], we assume $\alpha = 0$. In an isotropic environment, the charge distribution is uniform by definition. This is true for an ideal isotropic crystal and, given some time average, for a bulk isotropic crystal at finite temperature or a bulk liquid. As such, inhomogeneity corrections are negligible in any isotropic environment so they do not change most predictions of material properties used in the original fit for many EAM function sets. Since $|\nabla \rho_i| \neq 0$ near surfaces and other defects, β can be fit explicitly to corresponding experimental data. Furthermore, Eq. (1) is invariant under the transformations:

$$\begin{aligned} F_{i,c}(\rho_i) &= F_i(\rho_i) + c\rho_i, \\ \phi_{ij,c}(R) &= \phi_{ij}(R) - c\rho_i^a(R) - c\rho_j^a(R), \end{aligned} \tag{4}$$

where c is an arbitrary constant. Roelofs *et al.* point out that this invariance does not survive the addition of the term $\beta |\nabla \rho_i|^2$. Although they did not investigate transforming

 0031-9007/01/86(10)/2066(4)$15.00

functions, they suggest this as an additional route to improve the treatment of surface properties [5].

In this Letter, we test twelve EAM function sets for their ability to predict liquid/vapor surface tension γ. The sets are due to Foiles *et al.* [6,7], Voter and Chen [8], and Mishin *et al.* [9]; we refer to them as FBD, VC, and MFMP, respectively [10]. For FBD and VC, there are function sets for Al, Ni, Cu, Ag, and Au; for MFMP there are sets for Al and Ni. A wider range of charge density was explored during the fitting of both the VC and MFMP functions relative to FBD. Additionally, $\phi_{ij}(R)$ in FBD are purely repulsive which is not true for VC and MFMP. Function creation methodology for the three groups was sufficiently different to test its influence on γ prediction. In nearly all cases, model results for γ are significantly less than experiment. We show that results for γ can be improved by applying the $\beta|\nabla\rho_i|^2$ term in Eq. (3) and demonstrate that the degree of success obtained depends on aspects of the original function set, particularly the shape of $F_i(\rho_i)$. We also show that γ can be further improved in some instances by using Eq. (4) to alter the shape of $F_i(\rho_i)$. The effect of this correction on predictions of properties used in the original fit of the function sets, such as solid free surface and other defect energies, is discussed.

All simulations were performed in the isochoric-isothermal (NVT) ensemble with a Berendsen thermostat [11] and a time step $dt = 0.5$ fs. Each system began as an fcc crystal slab with dimensions $10a_0 \times 10a_0$ in the periodic surface plane and $8a_0$ thick. The slabs were melted and equilibrated for 1 ns; other temperatures were studied by reequilibrating the system for 250 ps. Data runs 1 ns in duration were then carried out for each T. The mechanical definition was used to calculate γ [12] and the statistical error was below 5% for all γ. Solid free surface energies were calculated by relaxing the relevant surface at $T = 5$ K for 50 ps and then gathering statistics over another 50 ps. Comparisons between our results and prior solid surface calculations [6,13] indicate this method is sufficient.

For calculations including the $\beta|\nabla\rho_i|^2$ term, the correction should be negligible in any isotropic environment. For an ideal crystal at finite T, the instantaneous $\nabla\rho_i$ for any atom oscillates about zero with an amplitude and period related to the atomic forces and state point. As such, $|\nabla\rho_i|$ and the accompanying correction are non-negligible, shifting the argument of F_i as much as 10%. Time averaging $\nabla\rho_i$ in both the bulk crystal and liquid states makes the correction from this term negligible ($<1\%$) after approximately 1 ps, similar to the period of oscillation of the system pressure. Because time averaging $\nabla\rho_i$ in the surface region does not change $|\nabla\rho_i|$ significantly, γ predictions within this approximation differed by less than 5% from those using the instantaneous $|\nabla\rho_i|$.

Figure 1 is a plot of γ for Al, Ni, Cu, Ag, and Au; results from simulation as well as experiment [14] are shown. Only for VC Al is there good agreement with experiment.

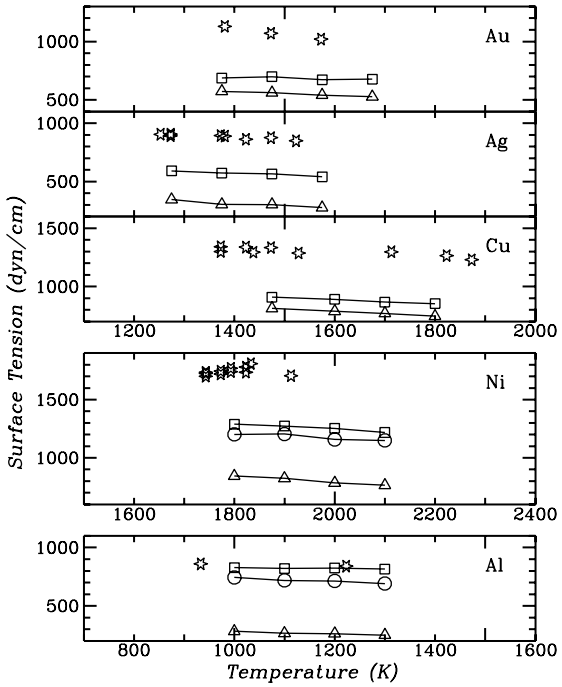

FIG. 1. Surface tension versus T for Al, Ni, Cu, Ag, and Au. Data are shown for FBD (triangles), MFMP (circles), and VC (squares), as well as experiment [14] (stars).

In the other cases, the experimental γ is underestimated by 20% to 60%. While ambiguity exists between experiments, the magnitude of this discrepancy is, in most cases, too large to attribute to anything but deficiencies in the models. However, qualitative features of the predictions agree well with experiment: the ordering of metals by γ is correct in all models and there is little dependence of γ on T. In all cases, VC performs best, followed by MFMP, and then FBD. This is similar to prior results for solid free surface energy calculations from these three models in that VC and MFMP perform distinctly better than FBD [6,9,13]. This is at least partly due to the methodology by which the respective groups generated their function sets.

To investigate adding corrections to the argument of F_i according to Eq. (3), Ni and Au in FBD and VC were studied. Results for γ for $\beta = -2.0$ to 2.0 are shown in Fig. 2. Equation (3) shows that the argument of F_i is increased for positive charge gradient corrections ($\beta > 0$). Data for Ni and Au show that positive gradient corrections improve the prediction of γ for VC. For VC Au, the response to the correction is fairly flat: at $\beta = 2.0$, the deviation from experiment has been reduced from 35% to 25%. For VC Ni, the response is much stronger so that, for $\beta = 0.5$, γ has increased 25%, reducing the deviation between model and experiment to less than 10%. Considering the variation in experimental data, this is acceptable. Increasing β for FBD is seen to decrease γ. Negative charge gradient corrections improve γ predictions for both Ni and Au in FBD. At $\beta = -2.0$ for Ni and -1.5 for Au, γ has increased 25% and 7%, respectively (FBD Au was unstable

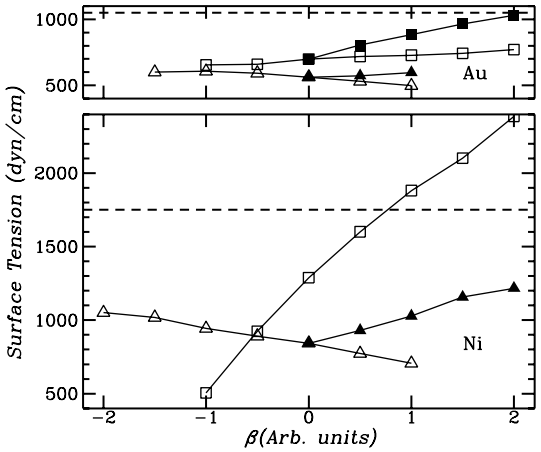

FIG. 2. Surface tension versus β for Ni ($T = 1800$ K) and Au ($T = 1475$ K) from FBD (triangles) and VC (squares). Open symbols show data for $c = 0$; closed symbols show data for transformed functions for Au in both FBD ($c = 400$) and VC ($c = 25$) and for Ni in FBD ($c = 325$). The horizontal dashed lines indicate the experimental value of γ.

for $\beta \lesssim -1.5$). The original predictions, however, are significantly less than experiment such that, even for Ni, the deviation between model and experiment is still 40% after correction. Similar results were obtained for other values of T.

The intent of the β correction is to penalize charge gradients so that defect structures, like surfaces, would be higher in energy. It is not implicit whether increasing or decreasing the argument of F_i will cause an energetic penalty due to the arbitrary nature of EAM functions. Observing the embedding functions and identifying the approximate value of charge density for atoms in the system clarify this. Figure 3 shows $F_i(\rho_i)$ for Ni and Au for both FBD and VC [we use the notation for untransformed embedding functions $F_i(\rho_i)$ in place of $F_{i,c}(\rho_i)$ when $c = 0$].

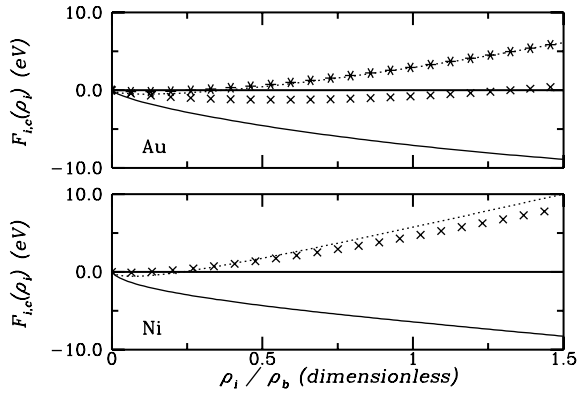

FIG. 3. $F_{i,c}(\rho_i)$ for Ni and Au in FBD (lines) and VC (symbols). Solid lines show FBD functions for $c = 0$; dashed lines show transformed FBD functions for $c = 325$ (Ni) and $c = 400$ (Au). VC functions are shown for $c = 0$ ($\times$) and, for Au, $c = 25$ ($*$). ρ_i for each model has been scaled by $\rho_b = 0.0375$, 0.3, 0.025, and 0.15 for FBD Ni, VC Ni, FBD Au, and VC Au, respectively.

Note that ρ_i in each case is scaled by the bulk value for that system ρ_b. For both VC metals, the relevant range of charge density $\rho_i/\rho_b \leq 1.0$ is a region of positive slope in $F_i(\rho_i)$. The opposite is true for FBD Ni and Au. Therefore, for VC an increase in energy is achieved by increasing the argument of F_i via $\beta > 0$. For FBD, an energetic penalty is achieved using $\beta < 0$.

The change in γ with β depends on both the magnitude of gradients in the surface and the local slope of $F_i(\rho_i)$. Equation (4) allows one to alter the slope of $F_i(\rho_i)$ giving $F_{i,c}(\rho_i)$. The sign of β which achieves an increase in γ is determined by the sign of the slope of $F_i(\rho_i)$. As such, a greater increase may be realized if the magnitude of the slope of $F_i(\rho_i)$ is increased. For VC functions this means using $c > 0$. Two options exist for FBD: $c < 0$ which makes the slope more negative or $c > 0$ but large enough to achieve a positive slope in the relevant ρ_i range. For the former option, $\beta < 0$ increases γ; however, as was already seen for FBD Au at $c = 0$ this can lead to system instability. With $\beta < 0$ the correction term can reduce the argument of F_i to zero so that an atom's energy is strictly determined by pair interactions. In FBD, $\phi_{ij}(R)$ is repulsive so completely eliminating contributions from the embedding term will create instability. As such, we use $c > 0$ and transform the FBD functions so that the $F_{i,c}(\rho_i)$ are similar to VC. In Fig. 3 we present transformed embedding functions $F_{i,c}(\rho_i)$ for FBD Ni along with $F_{i,c}(\rho_i)$ for Au in both FBD and VC. To demonstrate the effect of combining Eq. (3) with Eq. (4), in Fig. 2 we present γ versus β obtained by using transformed function sets (solid symbols). We use $c = 325$, 400, and 25 for FBD Ni, FBD Au, and VC Au, respectively. Since γ for VC Ni responded strongly to β for $c = 0$, we did not transform that function set.

Results for γ from transformed functions are identical to those from untransformed functions for $\beta = 0$. Figure 3 demonstrates that $F_{i,c}(\rho_i)$ for VC Au is more analogous to the original $F_i(\rho_i)$ for VC Ni. The transformation for VC Au results in a stronger response such that, for $\beta = 1.5$, the model prediction of γ has increased 40%, bringing it within 10% of experiment. For both FBD metals, the transformation is less successful. In fact, transformed FBD Au has a very limited range of β for which the system is stable and, within that range, there is no improvement of γ. FBD Ni does not show the same instability problems as Au in the range of β studied but, for $\beta = 2.0$, the model still underpredicts experiment by 30%. FBD employs a purely repulsive $\phi_{ij}(R)$ so that all attraction is provided by the embedding term. Increasing c gives rise to an attractive contribution to $\phi_{ij,c}(R)$. However, for c large enough to give transformed FBD embedding functions comparable to VC, $\phi_{ij,c}(R)$ has a minimum which is significantly deeper than for VC and located at separation distances significantly smaller than relevant interatomic spacings. Alternatively, using smaller c reduces the slope of $F_{i,c}(\rho_i)$. In either case, the benefit gained by

altering the argument of F_i is severely limited. For FBD Au, the transformed pair term results in large force contributions. For $\beta = 0$ these are exactly balanced by forces arising from the embedding term. But the balance is fragile and perturbations due to gradient corrections can destroy it, resulting in system instability. This instability can be controlled somewhat by reducing the time step. The data presented for transformed FBD Au in Fig. 2 were obtained with $dt = 0.25$ fs; at $dt = 0.5$ fs, $\beta = 1.0$ was unstable. However, the extension of stable β range and subsequent benefit gained for γ are not sufficient to warrant the smaller dt. VC is both more robust and responsive to the combination of transforming the functions and adding charge gradient contributions. Models for which charge gradient corrections work well have both an appreciable, positive slope for the embedding function and a corresponding pair term with a minimum near relevant interatomic spacings. VC is able to simultaneously meet these requirements, whereas FBD is not.

While we have improved the predictions of γ, it is important to test how other properties are altered by charge gradient corrections. Because of the form of the correction, there is no change for any environment which, on average, is isotropic. This is because the time average of $\nabla\rho_i$ is zero in an isotropic environment and the EAM is invariant to transformations such as those described by Eq. (4). As such, the only properties that can change are those associated with regions of net charge gradient. Since the most success was found for the VC parameter set, we tested the properties from their original fit that can change due to the introduction of gradient corrections: the unrelaxed vacancy formation energy E_v, the diatomic molecule bond length R_d, and energy E_d. We also tested the effect on the solid free surface energy E_s for the (100), (110), and (111) surfaces. For VC Ni, we tested ($c = 0$ $\beta = 0.5$) and for Au ($c = 25$ $\beta = 1.5$). Predicted E_s of the low index planes for VC Ni and Au increased in a fashion similar to γ. In addition, the original predictions of E_s were less than experiment by a similar magnitude as γ. As such, for these values of β and c, the average energy of the three planes differed from experiment by less than 10% for both Ni and Au. Results for R_d changed by less than 1%. The original deviation from experiment for E_d was 0.5% for both Ni and Au; with charge gradient corrections, the deviation is 2% for Ni and 3% for Au. The original fits of unrelaxed E_v matched experiment and, after relaxation, underpredicted experiment by 5%. The charge gradient correction increases energy in the presence of defects and, for unrelaxed E_v, this increase was fairly significant: 17% over experiment for Ni and 40% for Au. After relaxation, the deviation from experiment was less than 10% for Ni and roughly 25% for Au. The changes to the original fit data are, for the most part, small enough relative to the excellent improvement of γ and E_s predictions to warrant using charge gradient corrections, particularly for surface simulations. The significant effect on relaxed vacancy formation energy suggests that this should be weighed against surface energetics when optimizing β and c.

The use of charge gradient corrections in conjunction with appropriate EAM functions can provide surface property predictions in excellent agreement with experiment for solid and liquid metals. This extension of the EAM is only slightly more difficult to implement than the standard model and does not alter any predictions for isotropic environments. In the anisotropic cases so far examined, predictions using gradient corrections are either improved or altered little enough to warrant using this extension.

We acknowledge M. Baskes, S. Foiles, and A. Voter for helpful discussions. Sandia is a multiprogram laboratory operated by Sandia Corporation, a Lockheed Martin Company, for the United States Department of Energy under Contract No. DE-AC04-94AL85000.

[1] M. S. Daw, S. M. Foiles, and M. I. Baskes, Mater. Sci. Rep. **9**, 251 (1993).
[2] L. M. Holzman, J. B. Adams, S. M. Foiles, and W. N. G. Hitchon, J. Mater. Res. **6**, 298 (1991); B. Sadigh and G. Grimvall, Phys. Rev. B **54**, 15 742 (1996); M. Asta *et al.,* Phys. Rev. B **59**, 14 271 (1999).
[3] Jun Wan, Y. L. Fan, D. W. Gong, S. G. Shen, and X. Q. Fan, Model. Simul. Mater. Sci. Eng. **7**, 189 (1999).
[4] M. S. Daw, Phys. Rev. B **39**, 7441 (1989).
[5] L. D. Roelofs, S. M. Foiles, M. S. Daw, and M. I. Baskes, Surf. Sci. **234**, 63 (1990).
[6] S. M. Foiles, M. I. Baskes, and M. S. Daw, Phys. Rev. B **33**, 7983 (1986).
[7] S. M. Foiles and M. S. Daw, J. Mater. Res. **2**, 5 (1987).
[8] A. F. Voter, Los Alamos Unclassified Technical Report LA-UR 93-3901, 1993; A. F. Voter and S. P. Chen, Mater. Res. Soc. Symp. Proc. **82**, 175 (1987).
[9] Y. Mishin, D. Farkas, M. J. Mehl, and D. A. Papaconstantopoulos, Phys. Rev. B **59**, 3393 (1999).
[10] The potential for Al that we refer to as FBD was due to Foiles and Daw [7]. However, the methodology for creating the Al potential was nearly the same so, for convenience, the label FBD was used.
[11] M. P. Allen and D. J. Tildesley, *Computer Simulation of Liquids* (Clarendon, Oxford, 1987).
[12] W. Yu and D. Stroud, Phys. Rev. B **56**, 12 243 (1997).
[13] S. P. Chen and A. F. Voter, Surf. Sci. Lett. **244**, L107 (1991).
[14] R. C. Weast, *Handbook of Chemistry and Physics* (CRC Press, Boca Raton, FL, 1980), 61st ed.